Biochemical and Biophysical Research Communications 453 (2014) 148–152

Contents lists available at ScienceDirect

Biochemical and Biophysical Research Communications

journal homepage: www.elsevier.com/locate/ybbrc

Identification of an antitumor immune response of polyhistidine through a toll-like receptor 4-dependent manner

Feng Wang [a,b], Yong Yang [b,c,*]

[a] Department of Gastroenterology, The Tenth People's Hospital of Shanghai, Tongji University, Shanghai 200072, PR China
[b] Department of Nanomedicine, Houston Methodist Research Institute, Houston, TX 77030, USA
[c] Department of Medicine, Weill Cornell Medical College, New York, NY 10065, USA

ARTICLE INFO

Article history:
Received 12 September 2014
Available online 26 September 2014

Keywords:
Polyhistidine
Toll-like receptor 4
Single-molecule fluorescence imaging
Single-molecule force measurement
Cancer immunotherapy

ABSTRACT

Polyhistidine is widely used for the delivery of nucleic acids and antibodies into the cell cytoplasm. However, little attention has been concerned on the effect of polyhistidine on the immune system. In this work, we identify a novel function of polyhistidine as an activator of the immune system. Single-molecule fluorescence imaging and single-molecule force measurements show that polyhistidine binds specifically to the toll-like receptor 4 (TLR4), inducing receptor dimerization and activation. Moreover, in a B16 melanoma model we demonstrate that polyhistidine treatment inhibits tumor growth in $TLR4^{+/+}$ but not $TLR4^{-/-}$ mice. These results suggest the potential use of polyhistidine for cancer immunotherapy.

1. Introduction

Toll-like receptor (TLR) signaling is critical for the regulation of the innate and adaptive immune system, For instance, TLR signaling is involved in DC maturation, antigen presentation and CD8+ T-cell cytotoxicity, all of which are important for antitumor immunity [1,2]. The binding of an agonist to the TLR causes the homo/heterodimerization of TLRs, triggering the recruitment of intracellular adaptors that form signal transduction complexes in the cytoplasm. The formation of these complexes leads to the activation of signaling pathways, involving nuclear factor-κB (NF-κB), p38 mitogen-activated protein kinase (p38-MAPK) and c-Jun N-terminal kinase (JNK), which regulate the expression of genes involved in inflammation and immunity [3].

Bacterial and synthetic TLR agonists have been developed for cancer immunotherapy, and used either as single agents or in combination with tumor antigens. Such agonists have shown great promise for cancer treatment [4–10]. Here, we demonstrate the use of polyhistidine as a cheap alternative to conventional TLR agonists. We show that polyhistidine binds to TLR4, causing the activation of the immune system.

2. Materials and methods

2.1. Cells mice and reagents

High pure polyhistidine (100 monomers) was synthesized from SCILIGHT-PEPTIDE. TLR4 extracellular domain (TLR4-ECD) was purchased from Axxel Biosystem LLC. $TLR4^{+/+}$ and $TLR4^{-/-}$ DC2.4 dendritic cells were kindly provided by Dr. Kenneth Rock (University of Massachusetts Medical Center). B-16 melanoma cells were purchased from ATCC. Healthy C57BL/6 mice ($TLR4^{+/+}$ mice) were purchased from Charles Rive. TLR4 deficient C57BL/6 mice ($TLR4^{-/-}$ mice) were a kind gift from Dr. G. Nussbaum (Hebrew University). Total RNAs were extracted with the RNeasy mini kit from QIAGEN and reverse-transcribed by Superscript III from Invitrogen. Lipopolysaccharide (LPS) was purchased from Sigma. Primers for quantitative RT-PCR were obtained from Sigma. The TLR4 plasmid was purchased from Addgene, yielding the TLR4-green fluorescent protein (GFP) plasmid.

2.2. Cytokines and interferon responsive genes induction assays

Mice splenocytes were isolated from the spleen. Expression of cytokines and interferon responsive genes (IRG) were examined by quantitative RT-PCR. mRNA levels of cytokines, as well as a panel of IRG were quantified either after treatment with PBS, LPS (100 ng/mL), or polyhistidine (10 μM). LPS was used as a positive control.

* Corresponding author at: Department of Nanomedicine, Houston Methodist Research Institute, Houston, TX 77030, USA.
E-mail address: yyang@houstonmethodist.org (Y. Yang).

http://dx.doi.org/10.1016/j.bbrc.2014.09.078
0006-291X/

2.3. Quantitative RT-PCR

Quantitative RT-PCR was carried out as previously described [11]. RNA was extracted from the cells using RNeasy kit (QIAGEN). Total RNA (1 mg) was reverse transcribed into cDNA using Superscript III from Invitrogen in a 25 ml reactions. GAPDH served as endogens control. The following primer pairs were used:

IL-2 primers: forward primer: 5′-TGCAAACAGTGCACCTACTTCAA-3′; reverse primer: 5′-CCAAAAGCAACTTTAAATCCATCTG-3′.

IL-6 primers: forward primer: 5′-ATCCAGTTGCCTTCTTGGGACTGA-3′; reverse primer: 5′-TAAGCCTCCGACTTGTGAAGTGGT-3′.

IL-13 primers: forward primer: 5′-CTGTGAGCCTTGTCCTCCTC-3′; reverse primer: 5′-TTGGTGAGCCAGTGAGACG-3′.

TNFα primers: forward primer: 5′-CCTGTAGCCCACGTCGTAGC-3′; reverse primer: 5′-TTGACCTCAGCGCTGAGTTG-3′.

IFNβ primers: forward primer: 5′-CTGGAGCAGCTGAATGGAAAG-3′; reverse primer: 5′-CTTGAAGTCCGCCCTGTAGGT-3′.

IFNγ primers: forward primer: 5′-TGAACGCTACACACTGCATCTTGG-3′; reverse primer: 5′-CTCAGGAAGCGGAAAAGGAGTCG-3′.

STAT1 primers: forward primer: 5′-TTTGCCCAGACTCGAGCTCCTG-3′; reverse primer: 5′-GGGTGCAGGTTCGGGATTCAAC-3′.

OAS1 primers: forward primer: 5′-GGAGGTTGCAGTGCCAACGAAG-3′; reverse primer: 5′-TGGAAGGGAGGCAGGGCATAAC-3′.

MX1 primers: forward primer: 5′-GAATAGCAACTCCATACCGTG-3′; reverse primer: 5′-GTATTAAAGGTTGCTGCTAATG-3′.

ISG15 primers: forward primer: 5′-GTGGTGCAGAACTGCATCTC-3′; reverse primer: 5′-GCCAGAACTGGTCTGCTTGT-3′.

GAPDH primers: forward primer: 5′-TTCACCACCATGGAGAAGGC-3′; reverse primer: 5′-GGCATGGACTGTGGTCATGA-3′.

2.4. Cell culture and transfection

TLR4$^{+/+}$ and TLR4$^{-/-}$ DC2.4 cells were cultured in complete media comprised of RPMI-1640 (Gibco), supplemented with 10% FBS (Hyclone). Transfection was performed using FuGENE6 (Promega). Cells growing in a 35-mm glass-bottom dish (MatTek) were transfected with 0.3 μg/mL plasmids in the medium. To achieve a low-level protein expression, cells were incubated with the plasmid for 5 h, washed, and then imaged under the fluorescence microscopy. For the stimulation experiment, the transfected cells were added with LPS (100 ng/ml) or polyhistidine (10 μM) treatment in the medium for 30 min at 37 °C.

2.5. Single-molecule fluorescence imaging

Single molecule fluorescence imaging was performed with the objective-type total internal reflection fluorescence microscopy using an inverted microscope (IX 81, Olympus), a total internal reflective fluorescence illuminator, a 100X/1.45NA Plan Apochromat TIR objective (Olympus) and a 14-bit back-illuminated electron-multiplying charge-coupled device (EMCCD) (Andor iXon DU-897 BV). The microscope was equipped with a CO_2 incubation system (INU-ZIL-F1, TOKAI HIT) and all living cell imaging was performed at 37 °C in 5% CO_2. GFP was excited at 488-nm by an argon laser (Melles Griot) with the power of 5 mW measured after the laser passing through the objective in the epi-fluorescence mode. The collected fluorescent signals were passed through two filters, BA510IF and HQ 525/50 (Chroma Technology), before directed to the EMCCD. The gain of EMCCD was set at 300. As the intensity at the edge of illumination field of TIRFM was about 80% of that in the center, only the central quarter of the chip (256 × 256 pixels) was used for imaging analysis to ensure homogeneous illumination. Movies of 200 frames were acquired for each sample at a frame rate of 10 Hz using MetaMorph software (Molecular Device).

For the control experiment of single GFP molecule imaging on coverslip, GFP protein purified from *Escherichia coli* was firstly dissolved in the high salt buffer (600 mM NaCl, 150 mM PBS buffer, pH 7.4) to prevent the dimer formation and then immobilized on

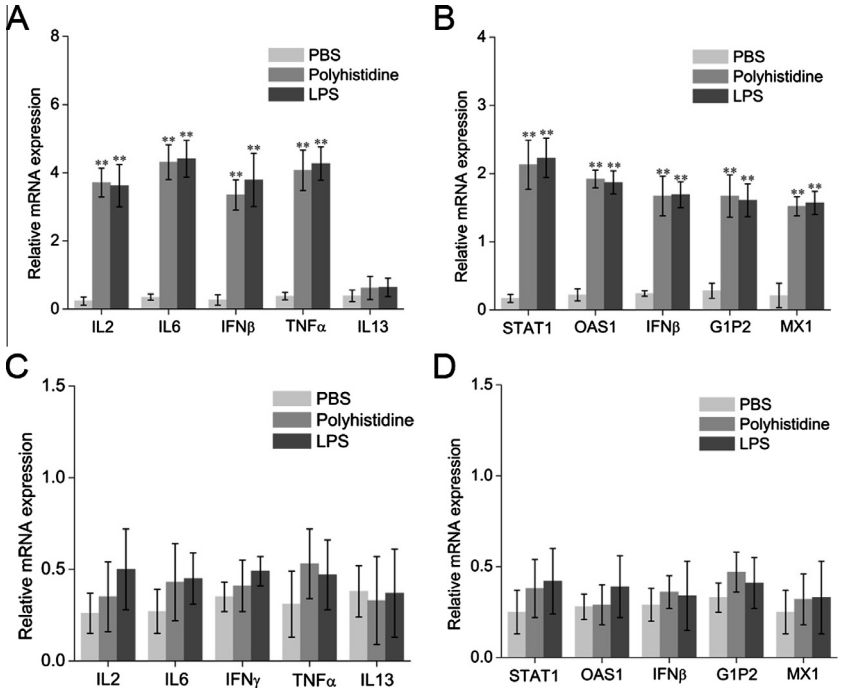

Fig. 1. Messenger RNA (mRNA) levels of cytokines and interferon response genes (IRGs) in splenocytes after exposure to polyhistidine. (A and B) Splenocytes harvested from toll-like receptor4 (TLR4)$^{+/+}$ C57BL/6 mice. (C and D) Splenocytes harvested from TLR4$^{-/-}$ C57BL/6 mice. Lipopolysaccharide (LPS) was used as a positive control for TLR4 activation. Data is plotted as the relative mRNA expression in comparison to glyceraldehyde 3-phosphate dehydrogenase (GAPDH). Data is expressed as mean ± SD. Statistical significance was measured by comparing experimental groups to the phosphate buffered saline (PBS) group. $^{**}P < 0.01$. IFNβ, interferon beta; IFNγ, interferon gamma; IL-2, interleukin 2; IL-6, interleukin-6; IL-13, interleukin 13; ISG15, ubiquitin-like protein ISG15; MX1, myxovirus resistance 1; OAS1, 2′-5′-oligoadenylate synthetase 1; STAT1, signal transducer and activator of transcription 1; TNFα, tumor necrosis factor alpha.

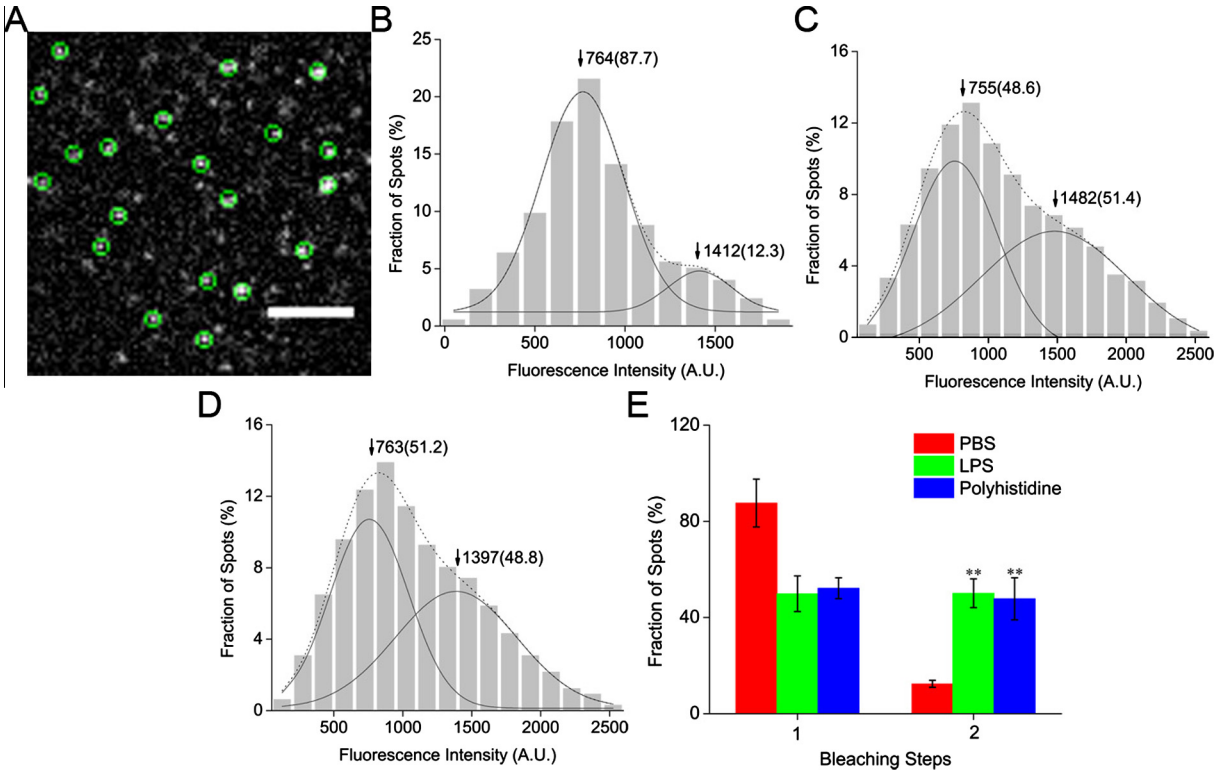

Fig. 2. Single-molecule fluorescence imaging of the toll-like receptor 4 (TLR4). (A) A typical single-molecule image of TLR4-green fluorescent protein (GFP) on the DC2.4 dendritic cell membrane. The spots enclosed by a green circle represent a signal from an individual TLR4-GFP molecule. Scale bar: 4 μm. (B–D) Distribution graph of the fluorescence intensity of individual TLR4-GFP spots from control cells (B), cells stimulated with LPS (C), and cells exposed to polyhistidine (D). The solid curves show the fitting of the Gaussian function, with the arrowheads indicating the peak positions. The two peaks represent a population of monomers and dimers, and the numbers in parentheses indicate the percentage of all counted spots. (E) Frequency of one- and two-step bleaching events. Data is expressed as mean ± SD. Statistical significance was measured by comparing the treatment groups to phosphate buffered saline (PBS). $^{**}P < 0.01$. (For interpretation of the references to colour in this figure legend, the reader is referred to the web version of this article.)

the coverslips through biotin coupled GFP antibody (Clontech) as previously reported [12].

For analysis of single-molecule fluorescence intensity in a movie acquired from living cells, the background fluorescence was first subtracted from each frame using the rolling ball method in Image J software (NIH). Then the first frame of each movie was used for fluorescent spot (regions of interest) selection. The image was thresholded (four times of the mean intensity of an area with no fluorescent spots), then filtered again with a user-defined program in Matlab. The fluorescent spots were selected as the previous report [12].

To analyze the bleaching steps, regions of interest for bleaching analysis were selected according to the method previously reported [13]. The background fluorescence was subtracted from the movie acquired from the fixed cells using the rolling ball method in Image J software.

2.6. Single-molecule force measurement

AFM silicon nitride (Si_3N_4) tips (type: NP, Veeco) were used in the experiments. Chemical modification of AFM tips were carried out as previous reported [14]. The force measurements of the polyhistidine modified AFM tips on the living cells were carried out on a PicoSPM II with PicoScan 3000 controller and a large scanner (Molecular Imaging). The AFM scanner was mounted on an inverted fluorescence microscopy (Olympus IX71, Japan). The loading rate of Force measurements was 1.0×10^4 pN/s. The force curves measured in living $TLR4^{+/+}$ or $TLR4^{-/-}$ DC2.4 cells were recorded and analyzed by PicoScan 5 software (Molecular Imaging). All forces were measured with contact mode at room temperature.

2.7. Inoculation of tumor cells and subcutaneous administration of polyhistidine

B16 melanoma cells were prepared as described previously [6]. 5×10^5 B16 melanoma cells were inoculated subcutaneously into shaved lateral flanks of the $TLR4^{+/+}$ or $TLR4^{-/-}$ mice. The mice were given a suspension of 100 μl polyhistidine (7 mg/ml), LPS (5 μg/ml) or PBS subcutaneous injection once every 5 days from 1 day before tumor inoculation. The size of primary tumors was determined every 3 days using calipers. Tumor volume was calculated using the formula $V = (A \times B^2)/2$, where V is the volume (mm^3), A is the long diameter (mm) and B is the short diameter (mm) [15].

2.8. Statistical analysis

Data were measured by analysis of variance, followed by Student's t-test (Microsoft Excel) for multiple comparisons. Data were performed as mean ± SD.

3. Results and discussion

3.1. Polyhistidine activates the immune system through TLR4

To assess the potency of polyhistidine to activate the immune system, we profiled cytokine mRNA levels in mouse splenocytes. Splenocytes were selected as the experimental model of study as they are the reservoir of immune cells in the murine body. This reservoir is mostly comprised of B-lymphocytes, but also includes T cells and monocytes, thus representing both the innate and the adaptive arms of the immune system. Splenocytes harvested from C57BL/6 mice were exposed to phosphate buffered saline (PBS),

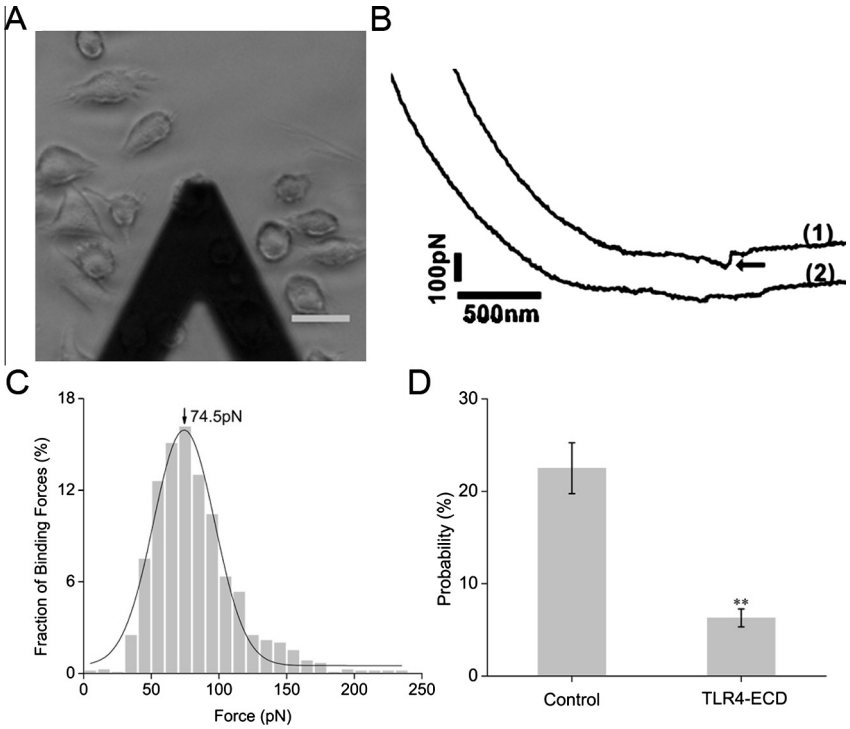

Fig. 3. Binding force measurements between toll-like receptor 4 (TLR4) and polyhistidine in DC2.4 dendritic cells. (A) An illuminated image of binding force measurements. Scale bar: 20 μm. (B) Force curves obtained in $TLR4^{+/+}$ cells (1) and $TLR4^{-/-}$ cells (2) using an AFM tip modified with polyhistidine. The arrowhead indicates the specific binding force between polyhistidine and TLR4. (C) Histogram of the binding forces between polyhistidine and TLR4 in $TLR4^{+/+}$ DC2.4 cells. The bars represent the experimental data, while the solid line is the theoretical Gaussian distribution curve. (D) The binding probability of polyhistidine to TLR4 in $TLR4^{+/+}$ cells with or without the blocking reagent (TLR4-ECD) treatment. Data is expressed as mean ± SD. Statistical significance was measured by comparing data obtained without TLR4-ECD treatment to data obtained with TLR4-ECD treatment. $^{**}P < 0.01$.

lipopolysaccharide (LPS) or polyhistidine for 2 h, where after the cells were washed and lysed. LPS, which is derived from the outer membrane of gram-negative bacteria, was used as a positive control, as it is an agonist of TLR4. Quantitative RT-PCR was employed to quantify the messenger RNA (mRNA) levels of various cytokines, including interleukin 2 (IL-2), interleukin-6 (IL-6), interleukin 13 (IL-13), tumor necrosis factor alpha (TNFα), interferon gamma (IFNγ), and the interferon responsive genes (IRG); 2′-5′-oligoadenylate synthetase 1 (OAS1), signal transducer and activator of transcription 1 (STAT1), interferon beta (IFNβ), myxovirus resistance 1 (MX1) and ubiquitin-like protein ISG15 (ISG15). The gene expression levels were normalized against the housekeeping gene glyceraldehyde 3-phosphate dehydrogenase (GAPDH). Fig. 1A illustrates that the expression levels of almost all of the above-mentioned cytokines increased approximately 10 to 14-fold in response to polyhistidine, reaching equal levels to that of the LPS control group. Similarly, expression of the IRGs increased 8 to 12-fold when exposed to polyhistidine (Fig. 1B).

However, the cytokine IL13 remained unchanged after treatment with polyhistidine or LPS. Previously, it has been shown that the levels of IL-13 increase in response to TLR2 activation but not TLR4 activation [16]. The observation that polyhistidine and LPS produce almost identical reactions in splenocytes suggests that polyhistidine may be an agonist for TLR4. To evaluate this notion, the expression levels of cytokines and IRGs were measured in splenocytes harvested from $TLR4^{-/-}$ C57BL/6 mice. Indeed, the results demonstrate the absence of an immune reaction in the splenocytes lacking TLR4 (Fig. 1C and D), indicating that the polyhistidine-induced immune response is TLR4 dependent.

3.2. Polyhistidine induces dimerization of TLR4

In order to study how polyhistidine activates the TLR4 signaling pathway, total internal reflection fluorescence microscopy (TIRFM) was employed. In particular, we studied receptor dimerization, which is a prerequisite for TLR4 activation and signal propagation

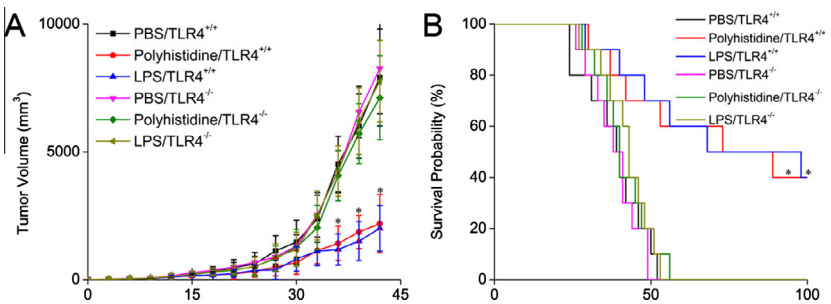

Fig. 4. Anticancer efficacy of polyhistidine in a subcutaneous B16 murine melanoma model. Toll-like receptor 4 $(TLR4)^{+/+}$ and $TLR4^{-/-}$ C57BL/6 mice received subcutaneous injection of PBS, polyhistidine or LPS. Tumor volumes (A, $n = 6$) and survival curves (B, $n = 10$) were recorded. Data are expressed as mean ± SD. Statistical significance was measured by comparing the polyhistidine or LPS $TLR4^{+/+}$ mice with the PBS $TLR4^{+/+}$mice. $^{*}P < 0.05$.

[17]. Prior to imaging, DC2.4 dendritic cells were transfected with a TLR4-green fluorescent protein (GFP) plasmid for 5 h. On the microscope images the TLR4-GFP molecules appeared as well-dispersed diffraction-limited fluorescent spots (5×5 pixels, 800×800 nm) (Fig. 2A and Supplementary Movie 1). The fluorescence intensity spots resembled a mix of two Gaussian distributions (Fig. 2B). The first distribution had a peak intensity close to that of a single GFP molecule, indicating the presence of TLR4 monomers (Fig. S1). The second distribution had a two-fold higher peak value, indicative of TLR4 dimers. A total of 373 fluorescent spots were counted, of which 87.7% were monomers and 12.3% were dimers. In response to LPS stimulation, the population of monomers decreased to 48.6%, while the population of dimers increased to 51.4% (Fig. 2C). This phenomenon suggests that LPS stimulation causes TLR4 receptor dimerization and activation.

In parallel, cells were treated with polyhistidine. The fluorescence intensity distribution in response to polyhistidine was similar to that obtained with LPS treatment (Fig. 2D). These results are consistent with the cytokine studies, supporting the notion that polyhistidine is an agonist to TLR4. To further confirm the presence of two distinct receptor populations, the TLR4 molecules were subjected to photobleaching (Fig. 2E). Bleaching-step counting is an emerging technique to determine the subunit number of membrane-bound proteins tagged to GFP [13]. The plots obtained with this approach reveal an LPS and polyhistidine induced increase of two-step photobleaching spots (Fig. S2A–B), hence, confirming the results obtained with the fluorescence distribution graphs.

3.3. Polyhistidine interacts with TLR4

To examine whether receptor dimerization was a consequence of polyhistidine binding to TLR4, live-cell single-molecule force spectroscopy was performed. Previously, this technique has been used to measure the binding force between ligand–receptor pairs [14]. Briefly, an atomic force microscopy (AFM) tip was modified with polyhistidine. The AFM tip was then moved in the vicinity of $TLR4^{+/+}$ or $TLR4^{-/-}$ DC2.4 cells (Fig. 3A) and the rupture force was detected as the tip broke contact with the cell (Fig. 3B). A substantial binding force could only be observed with $TLR4^{+/+}$ DC2.4 cells (Fig. 3C). Furthermore, blocking of the force with TLR4 extracellular domain (TLR4-ECD) solution was carried out to confirm that the measured forces were the specific ones between polyhistidine and TLR4 (Fig. 3D).

3.4. Polyhistidine inhibits tumor growth of B16 melanoma model

Previous reports have showed that TLR4 agonists are effective for the treatment of melanoma [18,19]. Therefore, we evaluated the antitumor efficacy of polyhistidine in a subcutaneous B16 murine melanoma model. Wild type C57BL/6 and $TLR4^{-/-}$ C57BL/6 mice received subcutaneous injection of PBS, polyhistidine or LPS. As shown in Fig. 4A, the tumor growth was significantly suppressed in the polyhistidine or LPS-treated $TLR4^{+/+}$ mice, but not in the $TLR4^{-/-}$ mice. All control mice died 55 days after cancer cell inoculation, whereas 40% of the polyhistidine or LPS-treated $TLR4^{+/+}$ mice survived beyond day 100 (Fig. 4B). Thus, the immunostimulatory effect of polyhistidine is evident both *in vitro* and *in vivo*.

In summary, we have discovered that polyhistidine is a TLR4 agonist and activator of the immune system. Single-molecule fluorescence microscopy and force spectroscopy results show that polyhistidine binds to TLR4, resulting in receptor dimerization. Furthermore, we demonstrate that polyhistidine can inhibit tumor growth in a murine melanoma model. Taken together, these results indicate that polyhistidine has the potential to be used for cancer immunotherapy. Our work also provides a promising method of using single-molecule techniques to exploit immune agonists for regulation of TLR signaling.

Acknowledgments

The authors acknowledge supports from the following funding source: Excellent Academic Backbone Program of Tenth People's Hospital of Shanghai (No. 12XSGG102)

Appendix A. Supplementary data

Supplementary data associated with this article can be found, in the online version, at http://dx.doi.org/10.1016/j.bbrc.2014.09.078.

References

[1] R. Medzhitov, Toll-like receptors and innate immunity, Nat. Rev. Immunol. 1 (2001) 135–145.
[2] N. Asprodites, L. Zheng, D. Geng, C. Velasco-Gonzalez, L. Sanchez-Perez, E. Davila, Engagement of Toll-like receptor-2 on cytotoxic T-lymphocytes occurs in vivo and augments antitumor activity, FASEB J. 22 (2008) 3628–3637.
[3] S. Akira, K. Takeda, Toll-like receptor signalling, Nat. Rev. Immunol. 4 (2004) 499–511.
[4] D. Reisser, A. Pance, J.F. Jeannin, Mechanisms of the antitumoral effect of lipid A, BioEssays 24 (2002) 284–289.
[5] I.H. Wolf, J. Smolle, B. Binder, L. Cerroni, E. Richtig, H. Kerl, Topical imiquimod in the treatment of metastatic melanoma to skin, Arch. Dermatol. 139 (2003) 273–276.
[6] Y. Kamiryo, T. Yajima, K. Saito, H. Nishimura, T. Fushimi, Y. Ohshima, Y. Tsukamoto, S. Naito, Y. Yoshikai, Soluble branched (1,4)-beta-D-glucans from acetobacter species enhance antitumor activities against MHC class I-negative and -positive malignant melanoma through augmented NK activity and cytotoxic T-cell response, Int. J. Cancer 115 (2005) 769–776.
[7] C.M. Paulos, A. Kaiser, C. Wrzesinski, C.S. Hinrichs, L. Cassard, A. Boni, P. Muranski, L. Sanchez-Perez, D.C. Palmer, Z. Yu, P.A. Antony, L. Gattinoni, S.A. Rosenberg, N.P. Restifo, Toll-like receptors in tumor immunotherapy, Clin. Cancer Res. 13 (2007) 5280–5289.
[8] C.M. Paulos, C. Wrzesinski, A. Kaiser, C.S. Hinrichs, M. Chieppa, L. Cassard, D.C. Palmer, A. Boni, P. Muranski, Z. Yu, L. Gattinoni, P.A. Antony, S.A. Rosenberg, N.P. Restifo, Microbial translocation augments the function of adoptively transferred self/tumor-specific CD8+ T cells via TLR4 signaling, J. Clin. Invest. 117 (2007) 2197–2204.
[9] S. Adams, Toll-like receptor agonists in cancer therapy, Immunotherapy 1 (2009) 949–964.
[10] S. Gnjatic, N.B. Sawhney, N. Bhardwaj, Toll-like receptor agonists: are they good adjuvants?, Cancer J 16 (2010) 382–391.
[11] Y. Yang, J. Wolfram, J. Shen, Y. Zhao, X. Fang, H. Shen, M. Ferrari, Live-cell single-molecule imaging reveals clathrin and caveolin-1 dependent docking of SMAD4 at the cell membrane, FEBS Lett. 587 (2013) 3912–3920.
[12] W. Zhang, Y. Jiang, Q. Wang, X. Ma, Z. Xiao, W. Zuo, X. Fang, Y.G. Chen, Single-molecule imaging reveals transforming growth factor-beta-induced type II receptor dimerization, Proc. Natl. Acad. Sci. USA 106 (2009) 15679–15683.
[13] M.H. Ulbrich, E.Y. Isacoff, Subunit counting in membrane-bound proteins, Nat. Methods 4 (2007) 319–321.
[14] J. Yu, Q. Wang, X. Shi, X. Ma, H. Yang, Y.G. Chen, X. Fang, Single-molecule force spectroscopy study of interaction between transforming growth factor beta1 and its receptor in living cells, J. Phys. Chem. B 111 (2007) 13619–13625.
[15] F. Wang, Y. Yang, Suppression of the xCT-CD44v antiporter system sensitizes triple-negative breast cancer cells to doxorubicin, Breast Cancer Res. Treat. (2014).
[16] D. Yang, Q. Chen, S.B. Su, P. Zhang, K. Kurosaka, R.R. Caspi, S.M. Michalek, H.F. Rosenberg, N. Zhang, J.J. Oppenheim, Eosinophil-derived neurotoxin acts as an alarmin to activate the TLR2-MyD88 signal pathway in dendritic cells and enhances Th2 immune responses, J. Exp. Med. 205 (2008) 79–90.
[17] H. Tsukamoto, K. Fukudome, S. Takao, N. Tsuneyoshi, M. Kimoto, Lipopolysaccharide-binding protein-mediated Toll-like receptor 4 dimerization enables rapid signal transduction against lipopolysaccharide stimulation on membrane-associated CD14-expressing cells, Int. Immunol. 22 (2010) 271–280.
[18] V. Andreani, G. Gatti, L. Simonella, V. Rivero, M. Maccioni, Activation of Toll-like receptor 4 on tumor cells in vitro inhibits subsequent tumor growth in vivo, Cancer Res. 67 (2007) 10519–10527.
[19] M.B. Davis, D. Vasquez-Dunddel, J. Fu, E. Albesiano, D. Pardoll, Y.J. Kim, Intratumoral administration of TLR4 agonist absorbed into a cellular vector improves antitumor responses, Clin. Cancer Res. 17 (2011) 3984–3992.